Comparative evaluation of the acceptor properties of quinone derivatized polypyridinic ligands

Ester Norambuena [a], Claudio Olea-Azar [d], Álvaro Delgadillo [b], Mauricio Barrera [c], Bárbara Loeb [c,*]

[a] Departamento de Química, Facultad de Ciencias Básicas, Universidad Metropolitana de Ciencias de la Educación, Santiago, Chile
[b] Departamento de Química, Facultad de Ciencias, Universidad de La Serena, Casilla 599, La Serena, Chile
[c] Facultad de Química, Pontificia Universidad Católica de Chile, Casilla 306, Santiago, Chile
[d] Facultad de Ciencias Químicas y Farmacéuticas, Universidad de Chile, Santiago, Chile

ARTICLE INFO

Keywords:
ESR
Electrophilicity index
Fukui function

ABSTRACT

The reduction properties of four acceptor polipyridyl ligands modified with quinones were studied by different experimental methods, as cyclic voltammetry and ESR spectroscopy, and by theoretical calculations. ESR spectra for the reduced ligands show different patterns among them, suggesting that the quinone moiety plays an important role in the delocalization of the received electron. The hyperfine coupling constants calculated for the magnetic nucleus were in good agreement with experimental data. The results were additionally interpreted with the help of two theoretical predictors: the electrophilicity index and the Fukui function obtained through the spin density. The results suggest that 12,17-dihydronaphtho-[2,3-h]dipyrido[3,2-a:2′,3′-c]-phenazine-12,17-dione, Aqphen, shows the most promising behavior to be employed as an acceptor ligand in complexes with potential application in NLO devices.

1. Introduction

The family of Ruthenium (II) polypiridyl complexes has been widely studied along the last 20 years due to their interesting basic properties as well as potential technological applications. In fact, by choosing the right combinations of ligands it is possible to tune the opto-chemicals properties of the complexes resulting in compounds with application in solar cells devices (SCD), organic light emitting devices (OLED) and in non linear optics (NLO). The latter field has been subject to increasing attention due to the pioneering work of Coe [1], Le Bozec [2], Frasier [3] and Green [4]. The nonlinear response of the polarizability in an electric field can be tuned by coordinating to the metal center two ligands possessing different acceptor and donor properties, enabling in this way the possibility of a charge separate state that generates a molecular dipole.

In order to be suitable for NLO devices the acceptor ligand must meet some basic requirements like (a) posses a planar geometry (b) show enhanced electron acceptor character. One way to predict if these requirements are present in a specific ligand, is to study the nature of the lowest unoccupied molecular orbital (LUMO), which reflects the electron withdrawing capacity and the electronic distribution in the acceptor state. However this is a virtual orbital and hence it cannot be accessed experimentally. This shortcoming can be overcomed by adding a single electron to this empty level, by means of the electrochemical reduction of the neutral molecule, giving rise to the single occupied molecular orbital (SOMO). The SOMO can be examined by two complementary approaches: one experimental, involving the reduction of the ligand and the subsequent analysis of the ESR pattern and hyperfine coupling constants, and the second, theoretical in nature, involving the calculation of suitable theoretical descriptors measuring the acceptor power and the delocalization of the unpaired electron along the molecular skeleton. The theoretical results would enable to construct a picture of the acceptor state and correlate it with the experimental data.

During the last years our group has focused part of its research on the synthesis and characterization of different quinone derivatized polypyridinic ligands with acceptor character, and their corresponding metal complexes: 12,17-dihydronaphtho-[2,3-h] dipyrido[3,2-a:2′,3′-c]-phenazine-12,17-dione, **Aqphen** [5,6], dipyrido[3,2-a:2′,3′-c]benzo [3,4]-phenazine-11,16-quinone, **Nqphen** [7], uracil(5,6-diamino-1,3-dimethyl), **Pptd** [8], Scheme 1.

All these ligands are rather planar and can be visualized as having a bidentate (N,N) phenanthroline type coordination center fused to a pyrazine or phenazine portion. Their difference lies on the type and relative position of the corresponding quinonic groups. Therefore, after receiving an electron, by direct reduction, or by MLCT (metal-ligand change transfer) excitation if forming part of a complex, they should behave as a "three step cascade" with a π^* ordering level following π^* (phenanthroline) > π^* (phenazine or pyrazine) > π^* (quinone portion) [5].

* Corresponding author. Tel.: +56 2 6864404; fax: +56 2 6864744.
E-mail address: bloeb@puc.cl (B. Loeb).

In this paper a comparative study of the three mentioned ligands, as well as the model ligand, pyrazino[2,3-f] [1,10]-phenanthroline, **ppl**, is presented and discussed. Emphasis is given to ESR spectroscopy and molecular calculations. The ligand **ppl** [9] was studied as a model, considering that it represents the unsubstituted fragment (Fig. 1) that can be modified by introducing three kinds of fragments containing quinonic groups: naphtoquinone, anthraquinone and dimethyl pyrimido quinone. The study is focused on the acceptor capacity of the ligand, and on the electronic density distribution on the SOMO, in order to predict its potentiality in applications as NLO.

2. Experimental section

All chemicals were reagent grade and used as received. The solvents used for synthesis were *p.a.* grade, while for electrochemical measurements spectroscopic grade solvents were used. All reagents (Aldrich) were *p.a.* grade and were used without further purification. Regarding the ligand synthesis, **Aqphen** and **Nqphen** were synthetized as described previously [5–7] while **Pptd** was synthesized according to Black and MacGuire. [8c] The model ligand **ppl** was also synthesized according to reported procedures [9].

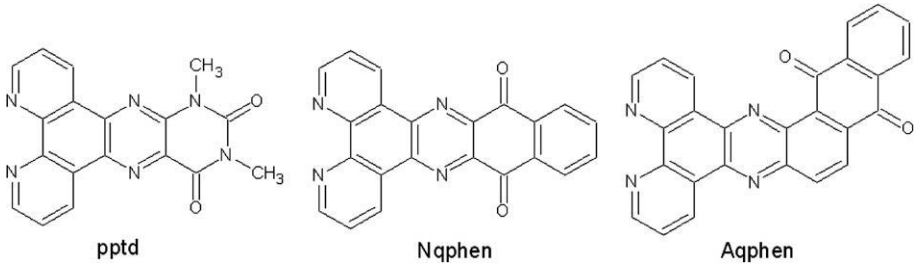

Scheme 1. Quinone derivatized polypyridinic ligands.

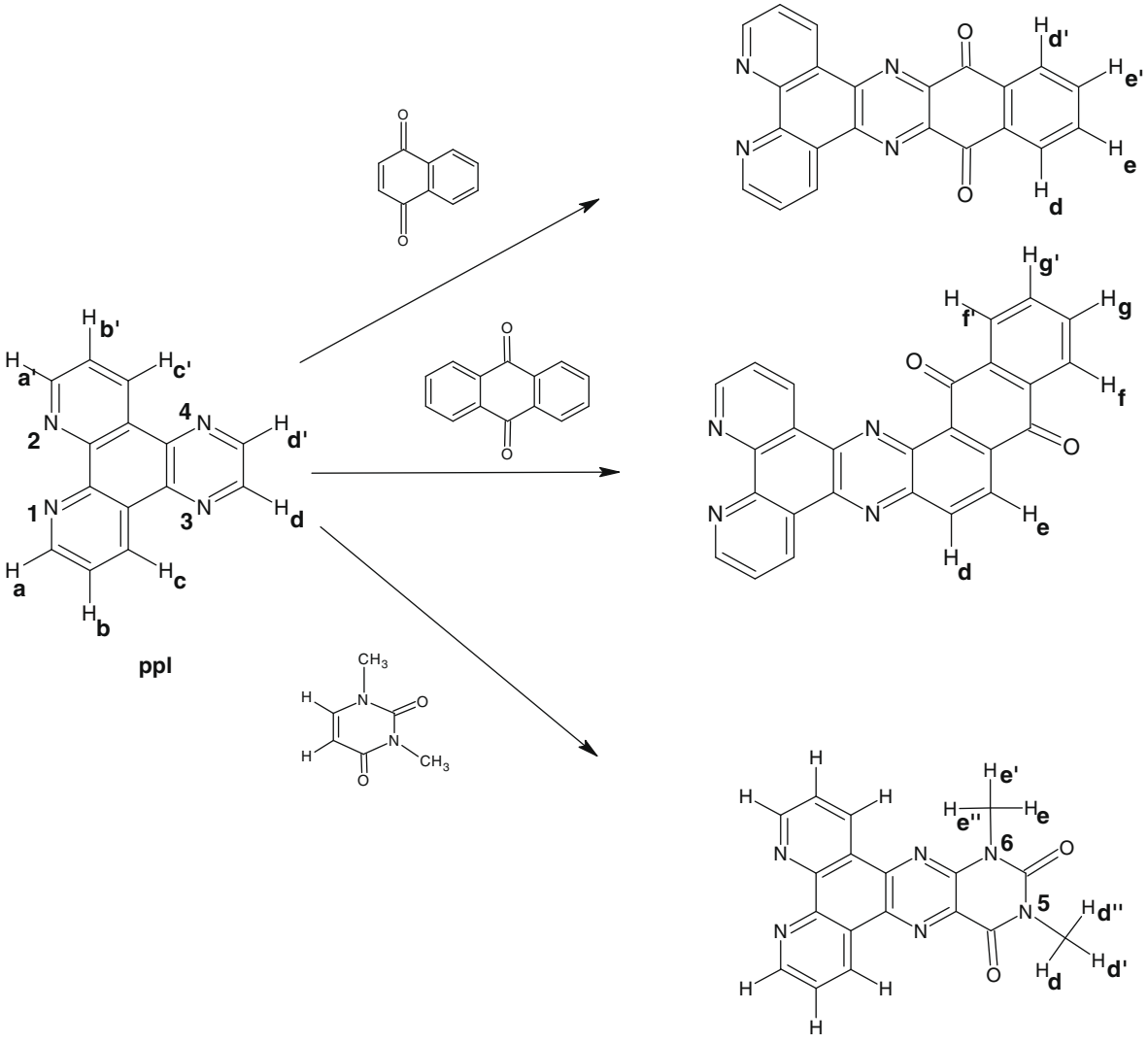

Fig. 1. Schematic *building* of the quinonic derivatized ligands starting from pyrazino[2,3-f][1,10]-phenanthroline (**ppl**).

Cyclic voltammetry measurements were carried out using a BAS 50 W potentiostat. A three electrode cell was employed using a platinum working electrode, an Ag/AgCl reference electrode and a platinum wire counter electrode. The potential of ferrocene/ferrocinium versus the Ag/AgCl reference is 0.35 V The experiments were performed in 0.1 M Bu_4NPF_6 in DMSO, acetonitrile or dichloroetane using a concentration of 1 mM of the ligands. The peak potentials given in the text are referenced to the SCE electrode. Electrochemical data for the **Pptd** ligand were taken from literature [8].

Isotropic ESR spectra were recorded in X band (9.85 GHz) using a Bruker ECS 106 spectrometer with a rectangular cavity and 50 KHz field modulation. DPPH (α,α'-diphenyl-β-picrylhydrazyl radical) was employed as reference for spectrum calibration. The radical anions were generated by electrolytic reduction "in situ" at room temperature. Other conditions of measurements were as follow: power: 20.1 mW, attenuation: 10.0 dB, modulation amplitude: 0.49 G, receiver gain: 1×10^5, conversion time: 40.96 ms, time constant: 81 ms. Each spectrum was recorded with 15 scans. The hyperfine splitting constants were estimated to be accurate within 0.05 G. Simulation of the ESR spectra was achieved using the software WINEPR Simphonia 2.11 version.

All calculations where performed using the ADF 2006.01 package [10]. Geometry optimizations where performed for all the ligands with the DZP basis set and PW91 exchange-correlation functional was employed. Two spin polarized calculations where performed with the LB94 corrected asymptotic decay exchange functional, with TZ2P basis set in order to compute the eigenvalues of neutral and the negative single charged ligand which correspond to the ionization potential ($-\varepsilon_{HOMO}$) and the electron affinity ($-\varepsilon_{SOMO}$). Hyperfine couplings constants were calculated with spin-polarization and TZ2P basis set. Three different exchange-correlations functional [11] were tested: OLYP, PBE and LB94. Whereas, for PBE, calculations have been reported [12], our results suggest that OLYP gives a better description of the spin density, and hence it will be employed for the calculations of the Fukui function. On the other hand, the LB94 exchange functional gives a poor description of the spin density on the hydrogen nucleus, but it is able to predict a bound state for SOMO eigenvalues that can be correlated with experimental data, like the first reduction potential of the neutral molecule.

3. Theoretical backgrounds

3.1. ESR

ESR still represents the simplest and probably the most useful experimental technique to directly detect and characterize free radicals with sufficient persistency to permit the acquisition of their ESR spectra. The property that allows to know the existing coupling between the unpaired electron and the magnetic nuclei present in the radical, and that is obtained from the ESR spectra, is the hyperfine coupling constant (a_i). In fact, it is worth recalling that the hyperfine coupling constant hfcc (a_i) arises from the Fermi contact interaction between the unpaired electron and the magnetic nucleus and is correlated to the corresponding spin density. The hfcc is the sum of the isotropic hfcc (Fermi contact) and anisotropic hfcc (dipole–dipole interactions). In isotropic solutions the dipolar interactions are averaged out, and therefore only the orientation-independent isotropic coupling is observed. Also, hfcc values could also be affected by geometric factors, such as bond length and bond angles. If the aromatic radicals are considered as being purely π systems, a simple formula provided many decades ago by Mc Connell permits to link the a_i on an atom with the spin density on the nearest magnetic nucleus: $a(i) = Q\rho_s(i)$, where Q is a constant that depends on the atom where the radical one is centered [13].

The ESR spectra of the different radical ions can be simulated by the program WINEPR Simphonia [14] using the experimental constants of hyperfine coupling, changing different parameters up to finding the major coincidence between the simulated spectrum with the experimental one. For the successful use of the simulation programs the introduction of starting hfcc values is needed, to be fitted in order to obtain a satisfactory correspondence with the experimental spectra. At the same time many computational packages are able to provide hfcc values from quantum chemical calculations: a combination of these two techniques is possible, and was used in this work.

3.2. Calculations

In the study of chemical reactivity the introduction of numerical parameters called "descriptors", that can be global or local", is important. The global descriptors consider the molecule as a whole, while the so called local descriptors explain the role of specific sites in the chemical skeleton that clarifies the selectivity of certain chemical reactions [15].

The focus of the present study aims in determining the increase in acceptor capacity of a polypiridyl ligand when quinonic substituent groups are added, and how an introduced charge will be distributed along the modified ligand. We propose that this behavior can be analyzed by means of a global descriptor as the electrophilicity index [16], that is a measure of the acceptor power of the neutral ligand, and the Fukui function [17], a local descriptor that shows how the spin density of the formed radical is distributed on the whole molecule. A brief description of both parameters is given below.

The capability of a ligand to accept one electron is measured by its electron affinity. However, if only partial electron transfer occurs, it is necessary to define a property taking into account the maximum electron flow that would lower the total binding energy. If an electrophilic ligand surrounded by a sea of electrons with zero chemical potential is considered, then an electronic flow will occur causing the increase of the chemical potential of the ligand until it becomes equal to the chemical potential of the sea. Hence the ligand will be saturated with electrons in an amount of $\Delta N_{max} = -\frac{\mu}{\eta}$ and the total energy has been lowered in

$$\Delta E = -E^+, \quad E^+ = \frac{\mu^2}{2\eta}, \tag{1}$$

where E^+ is the electrophilicity index [16] also known has "the electrophilic power", analogous to classical electricity where $W = V^2/R$. In the above equation, μ is the chemical potential, measuring the escaping tendency of the electrons and η, the hardness or the resistance of the species to liberate or accept electrons. Both properties can be further calculated in terms of the ionization potential (I) and the electron affinity (A):

$$\mu = \frac{1}{2}(I + A) \quad \text{and} \quad \eta = (I - A). \tag{2}$$

However most of the schemes fail in predicting a bound state for the Single Occupied Molecular Orbital (SOMO) eigenvalue; recent developments of new exchange functional including corrective terms for the long range behavior or by removing the self-interaction term [18] have opened the research field for highly charged molecules. Indeed, approximate expression for (2) in terms of the HOMO (ε_H) and LUMO (ε_L) eigenvalue, supported by Koopmans's Theorem [19] are currently employed

$$\mu = \frac{1}{2}(\varepsilon_H + \varepsilon_L) \text{ and } \quad \eta = (\varepsilon_H - \varepsilon_L). \tag{3}$$

Since the electrophilicity index is a global quantity giving information about the whole molecule, it is necessary for our ultimate purpose to specify how the accepted charge will be distributed along the different atoms of the molecule. This can be achieved by introducing a local descriptor like the Fukui function for a radical [20], $f_0(r) = \frac{\partial \rho(r)}{\partial N}$ which can be recast in terms of the condensed function [21],

$$f_\alpha = \rho_{S\alpha} = \rho_\alpha(\uparrow) - \rho_\alpha(\downarrow), \tag{4}$$

where $\rho_{s\alpha}$ is the spin density on atom α obtained through a Mulliken's population analysis. It follows that $\sum_\alpha f_\alpha = 1$ which is the normalized condition of the Fukui function.

The eletrophilicity index has been recently calculated for a series of organic free radicals [22]. Also the Fukui function for a radical has been defined as the response of the electronic density through a change in the spin polarization [23]. In both cases the focus was done in how the reactivity of the free radical would evolve upon eletrophilic or nucleophilic attacks. In the present work it is proposed that the use of these methods can be extended, in order that the frontier orbital of the free radical could be employed to describe the acceptor properties of the corresponding neutral molecule which is controlled by the LUMO orbital.

4. Results and discussion

4.1. Cyclic voltammetry

The model ligand, **ppl** exhibits a single reduction wave at −1.45 V vs. SCE in DMSO. This wave corresponds to a reversible diffusion-controlled one-electron transfer. No new waves appear in further scans out to −1.8 V. **Pptd** shows also a single quasi-reversible reduction wave at −0.84 V vs. SCE in DMSO; this wave was classified as quasi-reversible since the difference between the anodic and cathodic waves is 130 mV. **Nqphen** and **Aqphen**, on the other hand, present several reduction waves. For **Nqphen** three waves are observed at −0.65 V, −1.23 V and −1.53 V vs. SCE while for **Aqphen** two waves are reported at −0.5 V and −0.8 V vs. SCE. The first reduction wave for these compounds corresponds to a one-electron transfer and is attributable to the reduction of the quinone to its radical anion, while the other corresponds to the formation of the hydroquinone dianion.

4.2. ESR and theoretical analysis

The **ppl** free radical was prepared "in situ" by electrochemical reduction in DMSO, applying a potential corresponding to the first monoelectronic wave obtained from the cyclic voltammetric experiments (−1.45 V). The corresponding ESR spectrum (Fig. 2) shows high resolution. The unpaired electron interacts with four groups of two equivalent hydrogen nuclei producing four triplets. Additionally, the electron interacts with two equivalent groups of nitrogen's (3, 4) and (1, 2), that splits the signal in two quintets with coupling constants 6.03 and 0.33 G (Table 1).

The density functional methods are known for their capacity of providing reasonable predictions for ESR calculations of hyperfine coupling constants [24]. The interpretation of the ESR spectrum by means of a simulation process has led to the determination of the hyperfine coupling constants for all the magnetic nuclei. The values of these constants for the corresponding radicals for **ppl**, **Pptd**, **Nqphen** and **Aqphen** are shown in Tables 1–4.

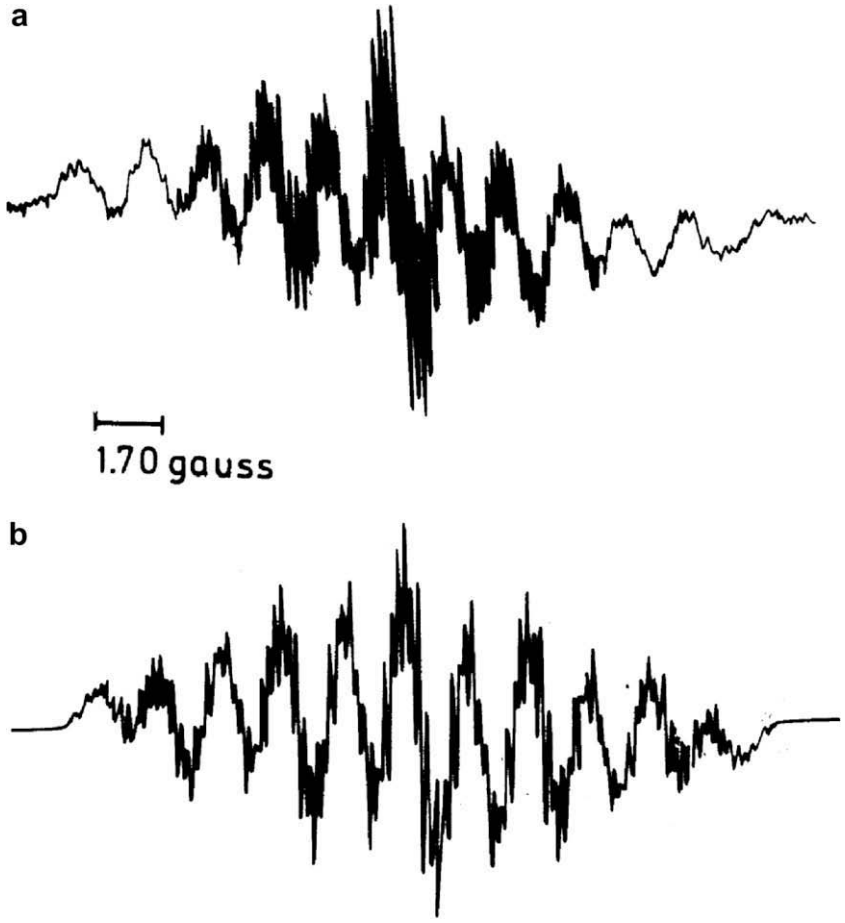

Fig. 2. ESR spectra of the ppl radical in DMSO a 25 °C. (a) Experimental spectrum; (b) simulated ESR spectrum; linewidth, 0.25 G and Lorentzian/Gaussian ratio of 0.4.

Comparing experimental values of hfcc with those predicted with OLYP and PBE on Table 1, we observe a good correlation among them; however, the high value of N3,4 cannot be reproduced by these methods,. On the other hand, LB94 reproduces this high value, but neglects the contribution of N1,2.

Fig. 3 shows values for the Fukui function in terms of the atomic component of the two fragments. According to this, the pyrazine fragment ($f = 0.55$) experiences a greater change in the electronic density than the phenantroline fragment ($f = 0.45$). Within the former fragment, the spin density is concentrated on nitrogen atoms (N3, N4) and carbons Cd, Cd' whereas for the case of the phenanthrolinic fragment, the spin density resides mainly over tertiary carbons with no hydrogen, and also over Cb, Cb' and Ca, Ca' [25].

Nqphen shows a different behavior. The monoelectronic reduction (Table 5) at −0.65 V indicates an increased reduction capacity in regard to **ppl**, and the formation of a drastically different radical. Table 2 shows the calculated values for the coupling constants, which are very small, practically negligible, as was also shown by the ESR experiment, suggesting that the unpaired electron is not located neither on the phenantroline nor on the pyrazine fragment. The explanation of these results is given in the next paragraphs.

Table 1
Experimental and predicted hyperfine coupling constants for the **ppl** radical, in G.

Magnetic nucleus	Coupling constants			
	Exp	OLYP	PBE	LB94
N 3,4	6.03	3.43	3.00	7.13
H d, d′	2.64	2.54	2.62	1.19
H a, a′	1.08	1.08	1.07	0.37
H b, b′	0.56	0.91	0.99	0.48
N 1, 2	0.33	0.29	0.34	0.03
H c, c′	0.13	0.19	0.23	0.32
g(iso)	2.002473			

Table 2
Predicted hyperfine coupling constants for the **Nqphen** radical, in G.

Magnetic nucleus	Coupling constants			
	Exp	OLYP	PBE	LB94
N 1,2	–	0.04	0.05	0.04
N 3,4	–	0.40	0.46	0.07
H a, á	–	0.63	0.66	0.22
H b, b́	–	0.11	0.12	0.03
H c, ć	–	0.53	0.54	0.20
H d, d́	–	0.13	0.13	0.06
H e, é	–	0.63	0.65	0.27

Table 3
Experimental and predicted Hyperfine Coupling Constants for the **Pptd** radical, in G.

Magnetic nucleus	Coupling constants			
	Exp	OLYP	PBE	LB94
N 3	4.66	3.84	3.11	8.53
N 4	2.60	2.33	1.89	5.36
H a	0.96	2.31	2.42	0.79
H c	0.93	1.56	1.48	0.39
Hd,d′,d″	0.87; 0.86; 0.86	0.82; 0.19	0.80; 0.18; 0.13	0.77; 0.18
N 6	0.99	0.29	0.29	0.33
N 1	0.26	0.35	0.34	0.13
N 2	0.24	0.29	0.02	0.01
N 5	0.20	0.19	0.23	0.28
g(iso)	2.003043			

Table 4
Experimental and predicted Hyperfine Coupling Constants for the **Aqphen** radical, in G.

Magnetic nucleus	Coupling constants			
	Exp	OLYP	PBE	LB94
H d	2.33	2.09	2.15	0.09
H a	1.10	0.71	0.63	0.20
N 3	1.20	1.13	1.0	2.34
N 4	0.98	1.11	0.97	2.43
Other Magnetic	Nucleuses	With	Minor	Constants Coupling
g(iso)	2.002614			

From Fig. 4 it is shown that the Fukui function has a 0.09 value on phenanthroline, 0.27 on pyrazine and 0.65 on the naphtoquinonic substituent. It is interesting to note that within this fragment most of the spin density is concentrated on the quinonic groups while for the pyrazine fragment, carbons atoms have accepted the incoming charge leaving the nitrogen atoms with no electron density.

For the **Pptd** ligand, the quinone moiety is in *meta* position instead of *para* as in **Nqphen**; the first consequence of this change in position can be observed on the reduction potential (Table 5) that moves from −0.65 to −0.84 V, showing that **Pptd** is more difficult to reduce than **Nqphen**. This trend is also reflected on the electrophilicity that drops from 6.44 in **Nqphen** to 4.58 in **Pptd** (OLYP),

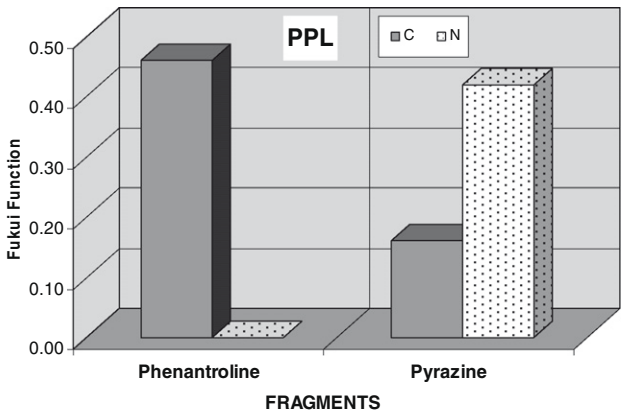

Fig. 3. Fukui function for the C, N, and O atomic components of the basic fragments for **ppl**.

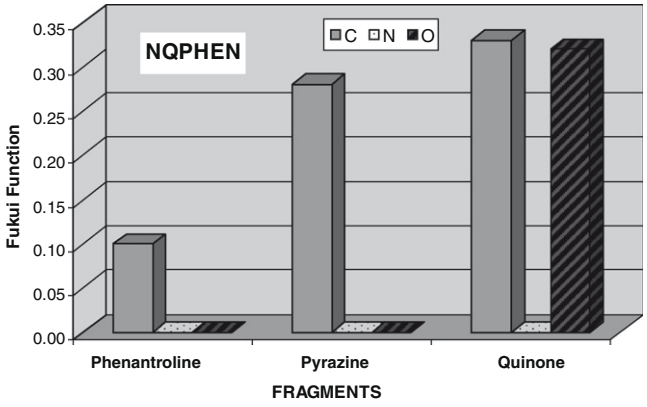

Fig. 4. Fukui function for the C, N, and O atomic components of the basic fragments for **Nqphen**.

Table 5
Electrophilicity index, Reduction Potential, and SOMO eigenvalue for several Ligands.

Ligand	E^+ (1)			E_{red} (2)	E_{somo} (1)
	OLYP	PBE	LB94		
Bipyridine	2.28	2.47	2.32		−3.32
Phenantroline	2.34	2.53	3.48		−3.48
Pyrazine	2.56	2.72	2.32		−1.96
ppl	3.31	3.65	4.37	−1.45	−4.29
Pptd	4.58	4.99	5.98	−0.84	−5.39
Nqphen	6.44	7.01	7.28	−0.65	−6.04
Aqphen	8.33	9.16	8.23	−0.50	−6.34
Naphtoquinone	6.31	6,97	5.19		−4.98
Anthraquinone	4.77	5.53	5.27		−5.01

(1) eV (2) volts.

while the SOMO eigenvalue is destabilized in 0.65 eV respect to **Nqphen**.

The ESR spectrum (Fig. 5) of the radical derived from **Pptd** was well resolved. These shows an hyperfine splitting with the highest spin density on one of the nitrogen nuclei of the pyrazinic part of the ligand, The unpaired electron interacts with each of the nitrogens, N1, N2, N3, N4, N5 and N6, producing six triplets; further interaction with the non equivalent hydrogen protons Ha, Hc splits the lines into two doublets, and the interaction with the remaining protons at CH_3 produces one new quartet (Table 3). Predicted values of hfcc for OLYP and PBE shows similar trends except for N4 and Ha, where OLYP predicts similar values, whereas if PBE is used, Ha has a higher spin density than N4. Finally, values for LB94 are too diverse, and were not analyzed.

The Fukui function for this ligand is displayed on Fig. 6; it shows a high value for the pyrazine fragment (0.63) with contributions from carbon (0.28) and nitrogen (0.35) atoms. It is interesting to note that the change in the relative position of the quinonic groups caused the charge to be redirected and stored on the nitrogen atoms of pyrazine.

The **Aqphen** is the ligand of the studied series that reduces most easily (−0.5 V); it also shows the highest electrophilicity index (Table 5) and the SOMO eigenvalue has moved to a lower value than **Pptd**, reflecting more stability and an increased charge acceptance capacity (Table 5). According to the theoretical calculations of the Fukui function shown in Fig. 7 for the **Aqphen** radical, the electronic density has experienced the higher change in the anthraqui-

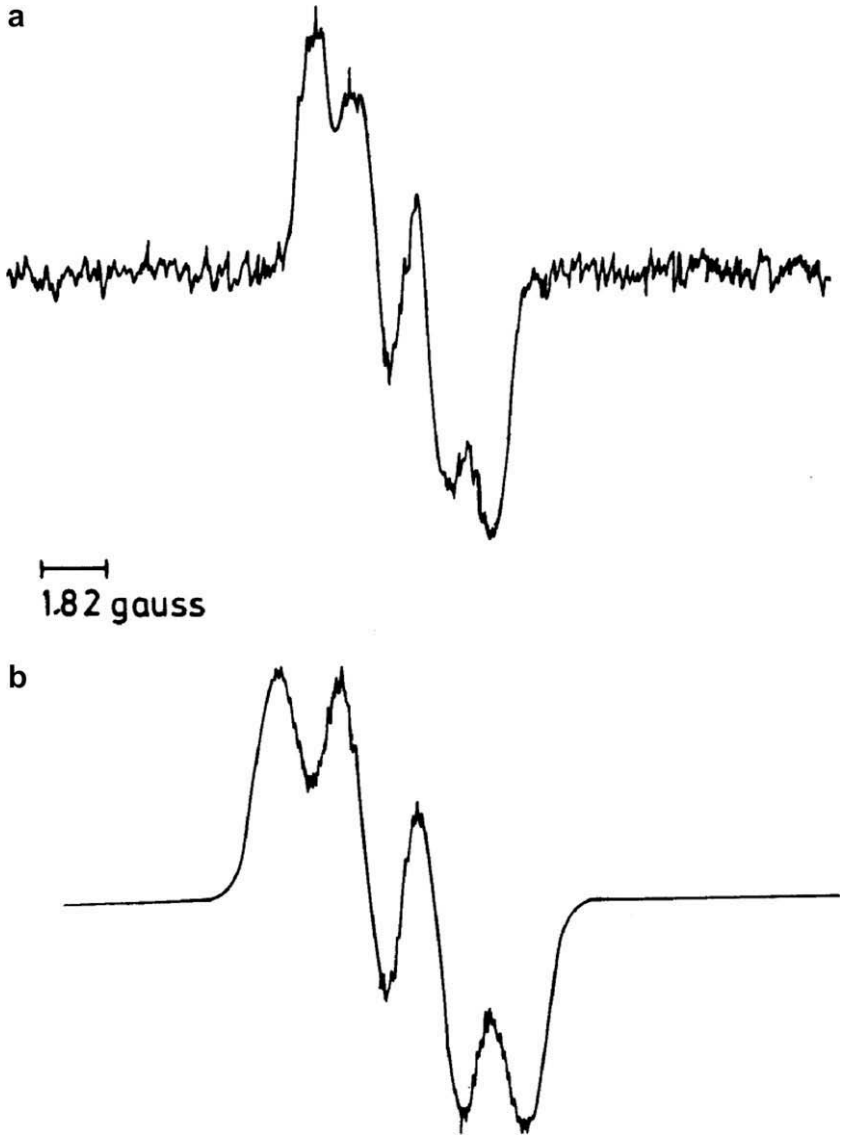

Fig. 5. ESR spectra of the **Pptd** radical in DMSO a 25 °C. (a) Experimental spectrum; (b) simulated ESR spectrum; linewidth, 0.25 G and Lorentzian/Gaussian ratio of 0.4.

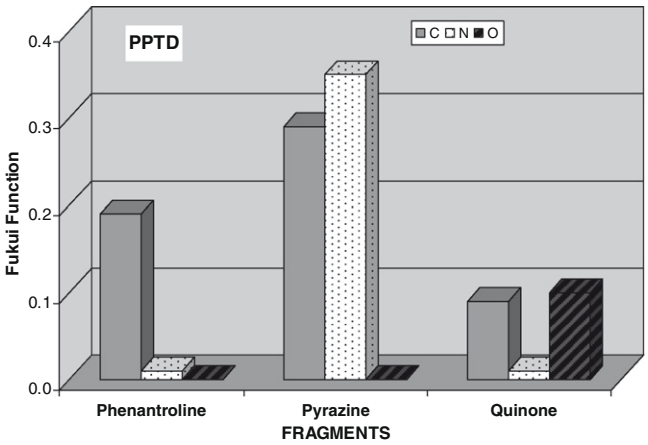

Fig. 6. Fukui function for the C, N, and O atomics components of the basic fragments for **Pptd**.

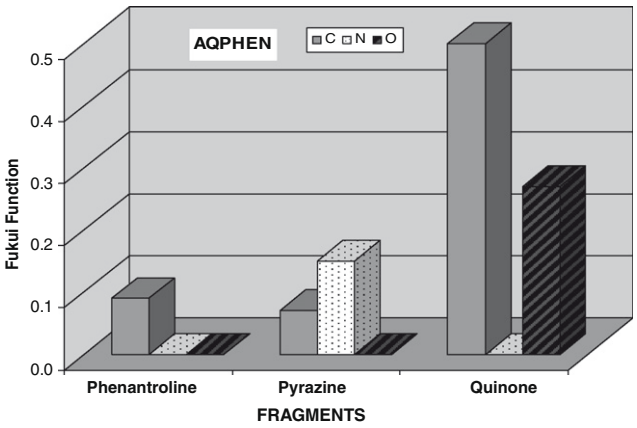

Fig. 7. Fukui function for the C, N, and O atomics components of the basic fragments for **Aqphen**.

nonic fragment (0.77) followed by the pyrazine (0.27) fragment upon the addition of the extra electron.

The hyperfine splitting on the EPR spectrum of the monoelectronic radical, obtained by electrochemical reduction, is shown in Fig. 8 and explained by the assignment for the constants given in Table 4. The unpaired electron interacts with two nitrogen's, N3 and N4, producing two triplet (isotropic value 1.20 and 0.98 G); further interaction with the protons H_a and H_d splits each line into two doublets (isotropic value 2.33 and 1.10 G).

From Table 4 it can be seen how the LB94 exchange functional predicts higher hfcc for nitrogen's nucleus from pyrazine, while experimental results, in conjunction with OLYP and PBE, show a different pattern with the hydrogen nucleus from the phenanthroline fragment exhibiting the higher coupling constants. Unlike **Nqphen**, where the nitrogen from pyrazine were not involved in the charge delocalization, **Aqphen** shows a collaborative effect between nitrogen atoms on pyrazine and the quinonic moiety, resulting in the enhancement of the electrophilic power of the whole molecule.

The above results suggest that in **Aqphen** the additional aromatic ring between pyrazine and naphtoquinone – giving rise to an anthraquinone fragment – may be responsible for electronic changes in the molecule that modify the local and the global properties in two ways; first, an enhancement of its acceptor character reflected by the electrophilicity index and the reduction potential. Secondly, the charge is moved away, far from the phenanthroline fragment containing the two nitrogens atoms that will coordinate the metallic center, therefore promoting charge separation as it was earlier proposed.

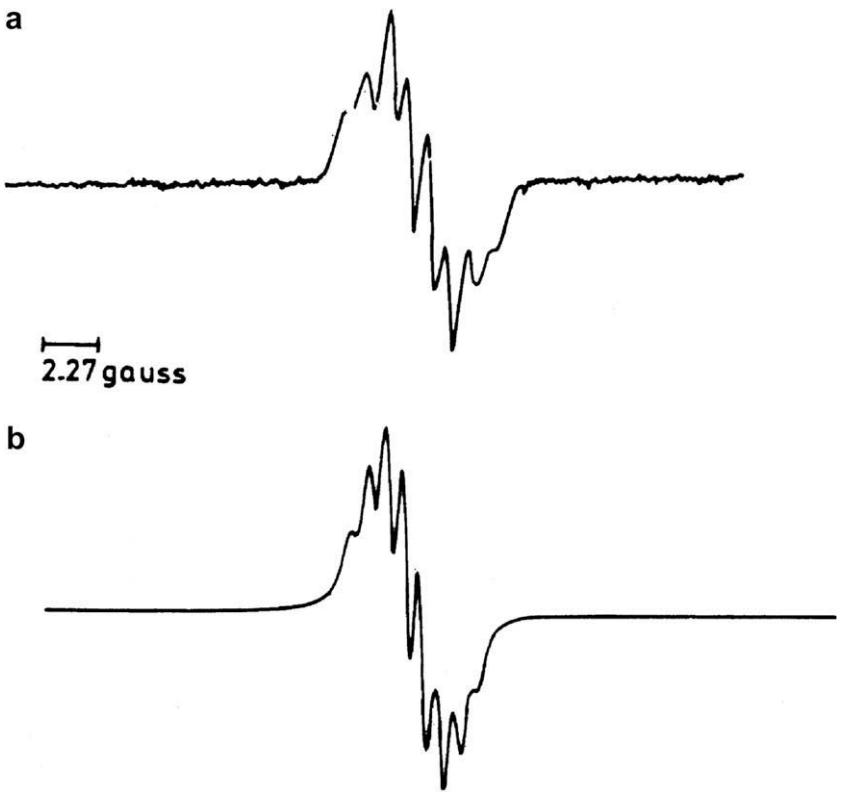

Fig. 8. ESR spectra of **Aqphen** radical in DMSO a 25 °C. (a) Experimental spectrum; (b) simulated ESR spectrum; linewidth, 0.8 G and Lorentzian/Gaussian ratio of 0.4.

Comparing the relative performance of the three exchange functional on predicting the hfcc it can be show that for N3,4 nucleus the average error for the three ligand using OLYP is 18%, for PBE is 26% and for LB94 is 90%. For the latte exchange functional, the error in the prediction of the hfcc of nucleus N3 increase with the size of the molecule: 18% (ppl), 83% (Pptd) and 95% (Aqphen). The same trend is found for N4. However for the case of OLYP and PBE the opposite tendency is observed. For example, for OLYP, the error on calculating the N3's hfcc follow the trend: 43% (ppl), 18% (Pptd) and 6% (Aqphen) and a similar decline is observed for PBE 50% (ppl), 33% (Pptd) and 17% (Aqphen).

Looking now at the results for hfcc on hydrogen nucleus (Ha, Hc and Hd) it is found the average error varies according to 43% (OLYP), 44% (PBE) and 62% (LB94).

In this sense, the above results suggest that OLYP exchange functional represents an improvement over PBE and LB94 when calculating hyperfine coupling constants.

Looking at Table 5 some interesting issues can be mentioned; first, a good correlation is observed between reduction potential, electrophilicity Index and the SOMO eigenvalue. Second, the SOMO eigenvalue is a good measure of the acceptor capacity of the corresponding ligand: the observed trend suggests that when the SOMO is stabilized the acceptor power increases, resulting in a molecule that is more easily reduced. It is important to note that the electrophilicity values obtained for the molecules under study are quite independent of the exchange functional used. However, for the specific case of pyrazine and anthraquinone, LB94 shows a different trend than PBE and OLYP. In general it can be mentioned that pyridine type compounds are worse electronic acceptors than aromatic quinones. Considering that the molecules under study can be decomposed in basic fragments the higher acceptor capacity of Aqphen and Nqphen can be explained if it is assumed that the overall electrophilicity value is the summation of the acceptor power of three dominant fragments: phenantroline, pyrarazine and a quinone containing fragment (Fig. 9).

On the other hand, the ESR experiments in conjunction with DFT methods proved to be a powerful tool to understand the electronic structure of the generated free radical. In this sense, the results suggest that OLYP exchange functional represents an improvement over PBE, when calculating hyperfine coupling constants. However, for the nitrogen nucleus, deviation from predicted hfcc respect to experimental values was observed; hence, the described methodology should be considered at a semi-quantitative level.

As a whole and looking at Fig. 9, it can be concluded that the electronic distribution is different for the acceptor polypiridinic ligand functionalized with quinonic groups depending if they are located in *meta* or *para* positions: in **Aqphen** and **Nqphen** the highest electron density is in the quinonic part. This is clearly reflected by the first reduction potential that appears at less negative potentials and the increasing value of the electrophilicity.

This behavior can be attributed to the electron withdrawing character of the quinonic moiety that contributes to the SOMO orbital. It also seems that an aromatic ring between the phenanthroline fragment and the quinone helps to increase the acceptor power of the ligand. Nevertheless, structural factors cannot be underestimated. The lineal nature of **Nqphen**, compared to the angled structure of **Aqphen**, can be responsible of the increased electron density on the quinonic moieties in the reduced form of the latter, compared to a more delocalized behaviour in the corresponding radical of **Nqphen**.

5. Conclusion

The combination of experimental (mainly ESR) and theoretical methods appear as a powerful tool to predict and compare the acceptor capacity of the series of ligands studied in this work. The use of the electrophilicity index – reported in literature mainly to predict reactivity of organic radicals – to describe the acceptor properties of the corresponding neutral ligands, showed to be particularly interesting. According to the mentioned theoretical and experimental data, and the analysis detailed in the preceding paragraphs, in the search of acceptor ligands to be used in Donor/Acceptor complexes for NLO applications, **Aqphen** shows advantage over the other studied ligands. This prediction will be tested by measuring the enhancement of the hyperpolarizability constant on acceptor–donor complexes containing this ligand. Regarding SCD applications, a carboxylic moiety must be introduced in the phenyl ring near the quinone in order to anchor the complex to the titanium dioxide surface. The action spectra of the supported complex will show how the new ligand influences electronic injection.

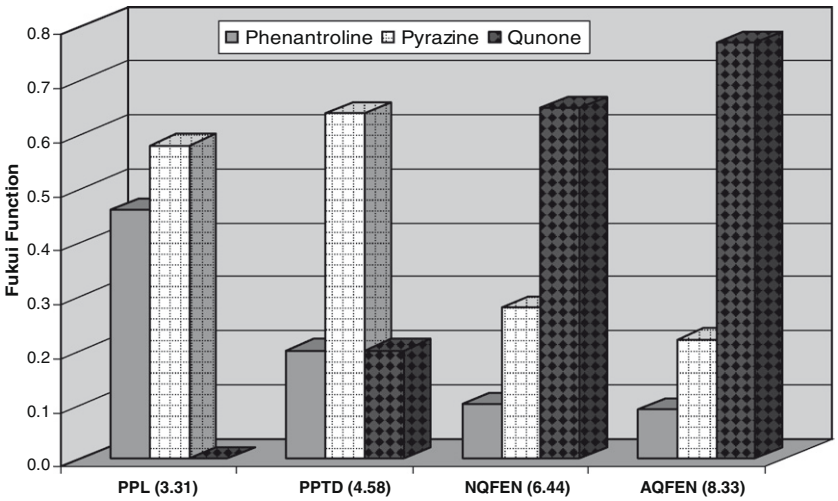

Fig. 9. Fukui functions for basic fragments and electrophilicity index for the series of acceptor ligands.

Acknowledgements

Fondecyt Grants 1020517 and 1070799 are gratefully acknowledged.

References

[1] B. Coe, in: J.A. McCleverty, T.J. Meyer (Eds.), Comprehensive Coordination Chemistry II, vol. 9, Elsevier-Pergamon, Oxford, 2004, p. 621.
[2] O. Maury, H. Le Bozec, Accounts of Chemical Research 38 (2005) 691.
[3] C.C. Frasier, M.A. Harvey, M.P. Cokerham, H.M. Hand, E.A. 0Chauchard, C.H. Lee, J. Phys. Chem. 90 (1986) 5703.
[4] M.L.H. Green, S.R. Marder, M.E. Thompson, J.A. Bandy, D. Bloor, P.V. Kolinsky, R.J. Jones, Nature 130 (1987) 360.
[5] R. López, A.M. Leiva, F . Zuloaga, B. Loeb, E. Norambuena, K.M. Omberg, J. Schoonever, D. Striplin, M. Deveney, T.J. Meyer, Inorg. Chem. 38 (1999) 2924.
[6] R. López, B. Loeb, T. Boussie, T.J. Meyer, Tetrahedron Lett. 37 (1996) 5437.
[7] R. Díaz, O. Reyes, A. François, A.M. Leiva, B. Loeb, Tetrahedron Lett. 42 (2001) 6463.
[8] (a) M. Saavedra, Licenciate in Chemistry Thesis, Pontifical Catholic University of Chile;
(b) M. Saavedra, A.M. Leiva, A. Carreño, R. López, M. Barrera, B. Loeb, unpublished work, in preparation;
(c) K. Black, H. Huang, S. High, L. Starks, M. Olson, M. Mc Guire, Inorg. Chem. 32 (1993) 5591.
[9] (a) .R. Díaz, A. François, M. Yañez, A.M. Leiva, B. Loeb, E. Norambuena, Helvetica Chim. Acta 89 (2006) 12;
(b) A. Delgadillo, P. Romo, A.M. Leiva, B. Loeb, Helvetica Chim. Acta 86 (2003) 2110.
[10] G. Te Velde, F. Bickelhaupt, E.J. Baerends, C. Fonseca Guerra, S. Van Gisbergen, J. Snijders, T. Ziegler, J. Comput. Chem. 22 (2001) 931.
[11] (a) R. van Leeuwen, E.J. Baerends, Phys. Rev. A 49 (1994) 2421;
(b) J.P. Perdew, K. Burke, M. Ernzerhof, Phys. Rev. Lett. 77 (1996) 3865;
(c) N. Handy, A. Cohen, Mol. Phys. 99 (2001) 403.
[12] E. Ionescu, A. Reid, J. Mol. Struct.: THEOCHEM 45 (2005) 745.
[13] H.M. McConnell, D.B. Chesnut, J. Chem. Phys. 28 (1958) 107.
[14] Bruker Win-EPR system. Copywrite 1990–1996. Bruker–Franzen Analytik 6 mbH. Version 2.11.
[15] T. Mineva, J. Mol. Struct.: THEOCHEM 762 (2006) 79.
[16] R. Parr, L. Szentpaly, S. Liu, J. Am. Chem. Soc. 121 (1999) 1922.
[17] (a) P. Fuentealba, R. Contreras, Reviews in modern quantum chemistry, in: K. Sen (Ed.), A Celebration of the contributions of Robert G. Parr., 2002;
(b) F. Fukui, Science 218 (1982) 747.
[18] M. Barrera, F. Zuloaga, J. Chilean Chem. Soc. 4 (2003) 27.
[19] R. Pearson, J. Chem. Ed. 64 (1987) 562.
[20] J. Gazquez, A. Vela, M. Galvan, in: K.D. Sen (Ed.), Electronegativity, Springer-Verlag, 1986. Structure and Bonding Series January.
[21] W. Yang, W. Mortier, J. Am. Chem. Soc. 121 (1986) 5708.
[22] F. De Viesschouvwer, V. Van Speybroeck, M. WAroquier, P. Geerlings, F. De Proft, Organics Lett. 9 (2007) 2721.
[23] E. Chamorro, J.C. Santos, C.A. Escobar, P. Perez, Chem. Phys. Lett. 431 (2006) 210.
[24] P. Stipa, Chem. Phys. 323 (2006) 501.
[25] T. Koizumi, Y. Yokoyama, K. Morihashi, M. Nakayama, O. Kikuchi, Bull. Chem. Soc. Jap. 65 (1992) 2839.